

# An experimental model of chronic severe mitral regurgitation



Martha M. O. McGilvray, MSt, MD, MPHS,<sup>a</sup> Tari-Ann E. Yates, MD,<sup>a</sup> Lynn Pauls, MD,<sup>b</sup> Meghan O. Kelly, MD,<sup>a</sup> Nicholas Razo, BS,<sup>c</sup> Stacie McElligott, BAS, RVTg, RLAT,<sup>a</sup> Glenn J. Foster, RT(R, MR),<sup>d</sup> Jie Zheng, PhD,<sup>e</sup> Jonathan K. Zoller, MD,<sup>b</sup> Christian Zemlin, PhD,<sup>c</sup> and Ralph J. Damiano, Jr, MD<sup>a</sup>

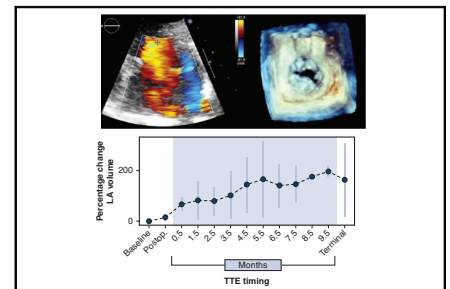
## ABSTRACT

**Objective:** To develop a minimally invasive, reproducible model of chronic severe mitral regurgitation (MR) that replicates the clinical phenotype of left atrial (LA) and left ventricular dilation and susceptibility to atrial fibrillation.

**Methods:** Under transesophageal echocardiographic guidance, chordae tendinae were avulsed using endovascular forceps until the ratio of regurgitant jet area to LA area was  $\geq 70\%$ . Animals survived for an average of  $8.6 \pm 1.6$  months (standard deviation) and imaged with monthly transthoracic echocardiography (TTE). Animals underwent baseline and preterminal magnetic resonance imaging. Terminal studies included TTE, transesophageal echocardiography, and rapid atrial pacing to test inducibility of atrial tachyarrhythmias.

**Results:** Eight dogs underwent creation of severe MR and interval monitoring. Two were excluded—one died from acute heart failure, and the other had resolution of MR. Six dogs underwent the full experimental protocol; only one required medical management of clinical heart failure. MR remained severe over time, with a mean terminal regurgitant jet area to LA area of  $71 \pm 14\%$  (standard deviation) and regurgitant fraction of  $52 \pm 11\%$ . Mean LA volume increased over 130% (TTE:  $163 \pm 147\%$ ,  $P = .039$ ; magnetic resonance imaging:  $132 \pm 54\%$ ,  $P = .011$ ). Mean left ventricular end-diastolic volume increased by  $38 \pm 21\%$  ( $P = .008$ ). Inducible atrial tachyarrhythmias were seen in 4 of 6 animals at terminal surgery, and none at baseline.

**Conclusions:** Within the 6 dogs that successfully completed the full experimental protocol, this model replicated the clinical phenotype of severe MR, which led to marked structural and electrophysiologic cardiac remodeling. This model allowed for precise measurements at repeated time points and will facilitate future studies to elucidate the mechanisms of atrial and ventricular remodeling secondary to MR and the pathophysiology of valvular atrial fibrillation. (JTCVS Techniques 2023;20:58-70)



A canine model of chronic severe mitral regurgitation showed marked cardiac remodeling.

## CENTRAL MESSAGE

This minimally invasive canine model replicated the phenotype of clinical severe mitral regurgitation, with marked structural changes and increased susceptibility to atrial tachyarrhythmias.

## PERSPECTIVE

This minimally invasive canine model replicated the phenotype of clinical severe mitral regurgitation. The left atrium and left ventricle underwent marked structural changes, with pronounced increases in both diameter and volume. This model successfully produced the valvular atrial tachyarrhythmia (ATA) substrate, with ATAs inducible in two thirds of animals.

The most recent available data estimate that primary mitral regurgitation (MR) affects approximately 24.2 million people internationally and more than 5 million in the United

States.<sup>1-4</sup> Atrial fibrillation (AF) is the most common cardiac arrhythmia,<sup>2</sup> and valvular disease is the most common worldwide cause of longstanding persistent AF.<sup>5</sup> In an

From the <sup>a</sup>Division of Cardiothoracic Surgery, Department of Surgery, and <sup>b</sup>Division of Cardiothoracic Anesthesiology, Department of Anesthesiology, Washington University School of Medicine, Barnes-Jewish Hospital, St. Louis, Mo; <sup>c</sup>Division of Cardiothoracic Surgery, Department of Surgery, <sup>d</sup>Center for Clinical Imaging and Research, and <sup>e</sup>Mallinckrodt Institute of Radiology, Washington University School of Medicine, St. Louis, Mo.

Supported by the National Institutes of Health RO1-HL032257 to R.J.D.; T32-HL007776 to R.J.D., M.M.O.M., and M.O.K.; and the Barnes-Jewish Foundation. Read at the 103rd Annual Meeting of The American Association for Thoracic Surgery, Los Angeles, California, May 6-9, 2023.

Received for publication Dec 31, 2022; revisions received March 10, 2023; accepted for publication March 22, 2023; available ahead of print May 6, 2023.

Address for reprints: Ralph J. Damiano, Jr, MD, Division of Cardiothoracic Surgery, Department of Surgery, Washington University School of Medicine, Barnes-Jewish Hospital, Campus Box 8234, 660 S. Euclid Ave, St. Louis, MO 63110 (E-mail: [damianor@wustl.edu](mailto:damianor@wustl.edu)).

2666-2507

Copyright © 2023 The Author(s). Published by Elsevier Inc. on behalf of The American Association for Thoracic Surgery. This is an open access article under the CC BY-NC-ND license (<http://creativecommons.org/licenses/by-nc-nd/4.0/>).

<https://doi.org/10.1016/j.xjtc.2023.03.027>

**Abbreviations and Acronyms**

AF	= atrial fibrillation
ATA	= atrial tachyarrhythmia
BSA	= body surface area
EDV	= end-diastolic volume
EF	= ejection fraction
HF	= heart failure
LA	= left atrium
LAA	= left atrial area ratio
LAV	= end-systolic left atrial volume
LV	= left ventricle
LVEF	= left ventricular ejection fraction
LVID	= end-diastolic left ventricular internal diameter
MR	= mitral regurgitation
MRI	= magnetic resonance imaging
RF	= regurgitant fraction
RJA	= regurgitant jet area
SD	= standard deviation
SV	= stroke volume
TEE	= transesophageal echocardiography
TTE	= transthoracic echocardiography

observational study of medically managed patients with primary MR in sinus rhythm at time of diagnosis, up to 48% of patients developed AF by 10 years.<sup>6</sup>

In order to study the physiological effects of MR on the heart, several groups have developed large animal models that reproduce the pathophysiology of MR to various degrees by rupturing the chordae tendinae of the mitral valve. The majority of these models were developed before the ubiquitous use of echocardiography and based their assessment of the severity of induced MR on acute catheter-based hemodynamic changes.<sup>7-13</sup> Only two groups made use of echocardiography at the time of MR creation to gauge severity—one using transthoracic echocardiography (TTE) and one using transesophageal echocardiography (TEE)—but neither listed any specific criteria.<sup>14,15</sup>

Many animal models of AF have also been developed, but the majority of these have not been reflective of the clinical picture of valvular AF, with methods such as rapid continuous pacing or pericarditis used to induce atrial arrhythmias.<sup>16,17</sup> While two groups have studied valvular AF in the more physiologic model of experimentally induced MR, both tested the inducibility of AF after only 1 to 3 months of regurgitation, potentially not allowing adequate time for development of the arrhythmogenic-substrate.<sup>14,15</sup>

Our aim was to develop a minimally invasive large animal model of chronic severe MR with rigorous echocardiographic guidance and explicit criteria for MR severity, followed by close echocardiographic surveillance. Our goal was to create a model of MR in which the development of atrial and

ventricular structural and electrophysiological remodeling could be studied over a prolonged period of time.

**METHODS****Animal Choice and Use**

Adult purpose-bred mongrel dogs weighing between 23 and 29 kg at the time of MR induction were used. This animal was chosen given the close parallels between canine and human cardiac anatomy and physiology.<sup>18</sup> All study protocols were reviewed and approved by the Washington University School of Medicine Institutional Animal Care and Use Committee and were in compliance with the National Institutes of Health Guidelines for the Care and Use of Laboratory Animals.

**Study Design**

**Pilot Study.** A nonsurvival pilot study was used to develop the surgical technique for endovascular creation of reproducibly severe MR and to ensure that this would be survivable in the immediate perioperative period. Four animals underwent creation of acute MR followed by euthanasia to allow for immediate gross evaluation of valvular damage. After MR was created, animals' vital signs were observed for 60 minutes to assess for clinical stability and any signs of heart failure (HF) or respiratory failure.

**Chronic Study.** The chronic study consisted of 4 stages. In the first stage, all animals underwent baseline cardiac magnetic resonance imaging (MRI). The second stage—survival surgery—included baseline TTE and TEE, transvenous burst pacing to assess inducibility of atrial tachyarrhythmias (ATAs), TEE-guided creation of MR, and completion TTE and TEE. During stage 3, animals were monitored clinically with weekly physical examinations and echocardiographically with TTEs first at 2 weeks and then approximately every 4 weeks. Toward the end of this interval monitoring period, animals underwent repeat MRI. Stage 4, the terminal surgery, consisted of final TTE and TEE examinations followed by transvenous burst pacing to reassess ATA-inducibility.

**Operative Technique for Creation of MR via Chordae Avulsion**

General endotracheal anesthesia was induced with 6 to 8 mg/kg of intravenous propofol and maintained with 1% to 5% inhaled isoflurane via mechanical ventilation. A femoral cut-down was performed to facilitate the placement of arterial and venous catheters for hemodynamic and arterial blood gas monitoring. In chronic study animals, a 10-cm 6-French femoral venous sheath was placed to enable the introduction of a pacing catheter for baseline assessment of ATA inducibility (described below section “Catheter-Based Evaluation of ATA Inducibility”). Before arterial access, animals were heparinized at a dose of 100 units/kg.

A right carotid cut-down was then performed, and a 10-cm 10-French access sheath was placed. Under fluoroscopic guidance and using over-the-wire technique, a 45-cm 7-French sheath was advanced into the left ventricular outflow tract. With this left ventricular outflow tract platform established, guidance was transferred to TEE. An endomyocardial biopsy forceps was advanced through the sheath and used to sequentially avulse the chordae tendinae of the mitral valve (Figure 1). MR was considered sufficient once the regurgitant jet area (RJA)-to-left atrial area ratio (LAA; further description below section “Quantitative and qualitative assessment of MR”) was greater than or equal to 70%. This is an established criterion for severe MR in the veterinary literature.<sup>19</sup> Once sufficient MR was confirmed, all instrumentation was removed and the carotid artery, femoral artery, and femoral vein were ligated. Soft tissue and skin were approximated with absorbable suture; animals were extubated and recovered from anesthesia.

**Echocardiographic Examination and Analysis**

TEEs were performed during the survival and terminal surgeries with animals in either the supine or lateral decubitus position under general

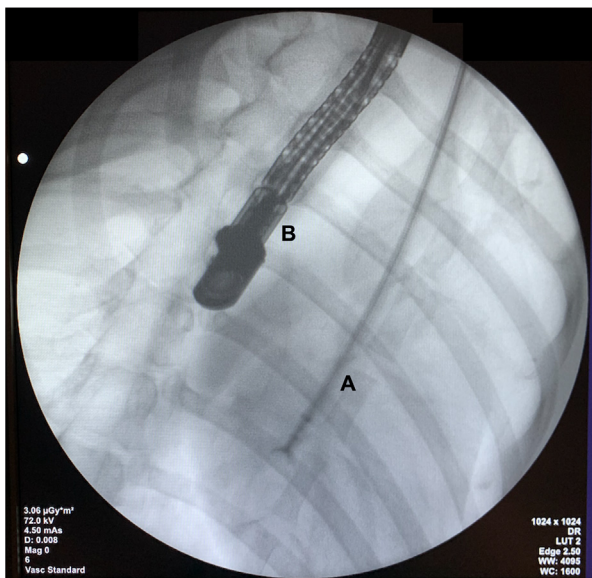


**FIGURE 1.** Representative fluoroscopic image of endovascular avulsion of mitral valve chordae tendinae using endomyocardial biopsy forceps. A, Biopsy forceps in the left ventricular outflow tract; B, transesophageal echocardiography probe in the esophagus.

anesthesia with propofol and isoflurane, as described previously. All TTEs were performed in the right and left lateral decubitus positions (see Figure 2 for representative echocardiographic images). Interval monitoring TTEs were performed without sedation in awake animals; TTEs performed during survival and terminal surgeries were performed under general anesthesia. Echocardiographic examinations were performed with either a SonoSite M-Turbo (Fujifilm SonoSite) or a Philips iE33 (Philips Healthcare), and analysis was performed using Synapse CardioVascular (Fujifilm Holdings Company America).

**Quantitative and qualitative assessment of MR.** MR was assessed both via TTE and TEE. On TTE examination, MR severity was primarily quantified via RJA/LAA, as measured in the left lateral apical windows. RJA and LAA were measured on the same still frame using color

Doppler with a Nyquist limit set between 50 to 70 cm/s. On terminal TEE examination, regurgitant fraction (RF) was calculated using the flow convergence via proximal isovelocity surface area method (see Appendix E1 material [Online Data Supplement]).<sup>20</sup>

**Definition of severe MR.** MR was classified as severe if any of the following findings were present on either TTE or TEE: evidence of a flail leaflet, an eccentric wall-impinging jet, or RJA/LAA >50%.<sup>20</sup> A greater threshold for RJA/LAA of 70% was used as the goal for MR creation during the survival surgery, given the possibility of remodeling and potential decrease in RJA/LAA over multiple months postoperatively.

**Structural remodeling assessment.** End-systolic left atrial volume (LAV) and end-diastolic left ventricular internal diameter (LVID) were measured via TTE, the former via a left apical 4-chamber view and the latter via a right parasternal mid-papillary short-axis view. Both were indexed to body surface area (BSA). BSA was calculated using the standard veterinary equation for BSA:

$$BSA = 10^{-4} \cdot K \cdot w^2$$

where  $K$  is a species-specific constant (canine  $K = 10.1$ ), and  $w$  is the weight of the animal measured in grams.<sup>21</sup> Left ventricular (LV) ejection fraction (EF) and stroke volume (SV) were calculated using measurements of end-systolic and end-diastolic left ventricular volumes as seen via TEE 2-chamber and 4-chamber views (see Appendix E1 [Online Data Supplement]). SV was indexed to BSA.

## MRI and Analysis

General endotracheal anesthesia was induced and maintained as described previously. Animals underwent magnetic resonance cine imaging using electrocardiogram-synchronized free-breathing 2D fast low-angle shot sequences on a 3-Tesla MRI scanner (MAGNETOM Prisma; Siemens Healthineers). Animals were imaged in the left lateral decubitus position. Long-axis 2-, 3-, and 4-chamber images and short-axis stack were obtained from just above the bilateral atria to just below the apex of the heart with the following parameters: repetition time/echo time 3.3 milliseconds/1.43 milliseconds; temporal resolution: 23.1 milliseconds, flip angle 12°; and spatial resolution: 0.8 × 0.8 × 0.8 mm. Images were analyzed using Medis Suite MR (Medis Medical Imaging Systems BV), with manually checked automated segmentation of the endocardium and epicardium of the LA and LV. LVEF was reported as a direct calculation; LV SV, LV end-diastolic volume (EDV), and LAV were indexed to BSA as described previously.

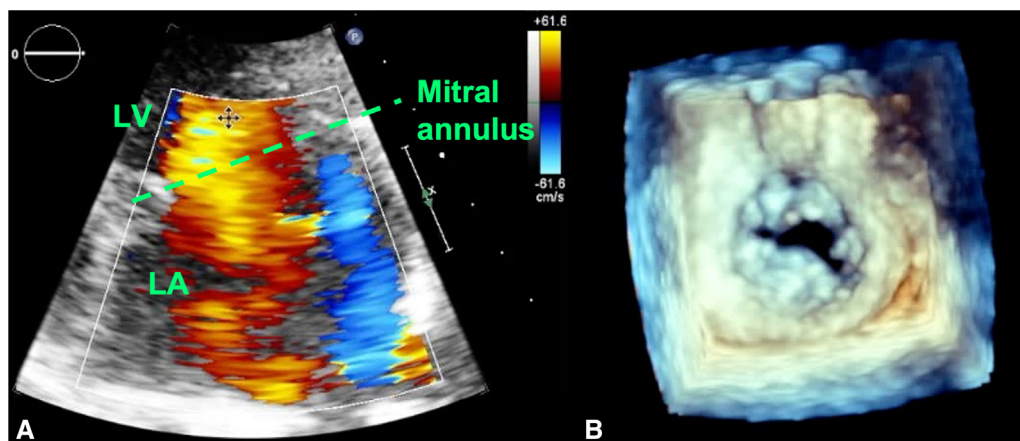


**FIGURE 2.** Representative echocardiographic images of severe mitral regurgitation (MR). A, Transthoracic echocardiographic image (apical 4-chamber view) of the left atrium (LA) with color Doppler showing eccentric MR jet with Coanda effect (wall-hugging, wrap-around jet). B, Transesophageal echocardiographic 3-dimensional image of the mitral valve en face, ie, surgeon's view, showing coaptation defect associated with flail leaflet, imaged during terminal surgery. LV, Left ventricle.

### Postoperative Animal Handling

During the interval monitoring period, animals were monitored for signs of HF—exercise intolerance or difficulty with lateral decubitus positioning as manifested by increased work of breathing or decreased peripheral oxygen saturation—via weekly physical examinations and monthly TTEs. If signs of HF were appreciated or impaired LV function was noted on monthly TTEs, animals were started on 3 mg/kg oral furosemide daily.

### Catheter-Based Evaluation of ATA Inducibility

In chronic study animals, ATA inducibility was assessed during the survival surgery (before MR creation) and during the terminal surgery. At the time of terminal surgery, general endotracheal anesthesia was induced and maintained as described previously, and the femoral vein not previously ligated was accessed either percutaneously under ultrasound guidance or via cut-down. A transvenous pacing catheter was introduced via a 10 cm 6-French sheath and advanced into the right atrial appendage. Placement was confirmed via observation of limb-lead electrocardiograms consistent with atrial activation during continuous pacing (amplitude 2 mA, period 300 milliseconds). During survival surgery, burst pacing was attempted 1 to 3 times with a 30-second burst at 1.5 to 2 mA and 100 milliseconds. During terminal surgery, burst pacing was attempted 1 to 6 times with a 30-second burst at 0.6 to 3 mA and 80 to 135 milliseconds (Figure 3). Each animal was considered to have an inducible ATA if they had at least one burst-initiated ATA lasting 30 seconds or longer.

### Statistical Analysis

Continuous variables were expressed as mean ± standard deviation (SD). Means of variables measured at baseline and at time of terminal surgery were compared using a paired-samples *t*-test. Percent change from baseline to time of terminal surgery was calculated for RJA/LAA, LAV (both TTE- and MRI-derived), LVID, and LV EDV—with baseline defined as either presurvival surgery or immediately postsurvival surgery, as appropriate. The alpha value for all statistical tests was 0.05. All statistical analyses were performed using SAS Studio 3.8 on SAS 9.4 (SAS Institute Inc).

## RESULTS

### Pilot Study

A pilot study was performed to optimize the technique for MR creation and ensure acute survivability. Four animals were included in the nonsurvival pilot study (Table E1). All dogs met the criteria for severe MR with RJA/LAA >50% and a flail leaflet and/or an eccentric wall-impinging jet (Table E2). Mean RJA/LAA was  $74 \pm 14\%$  (SD). All animals remained hemodynamically stable after establishment of severe MR without any acute decompensation or change in respiratory status. This pilot study allowed for improved targeting of chordae immediately inferior to the posterior and anterior leaflets or immediately superior to their papillary muscle insertion. Procedure duration and number of forceps-passes needed to obtain severe MR decreased over the short study, reflecting the learning-curve of the single surgeon performing the procedures.

### Chronic Study

**Perioperative outcomes and animal characteristics.** A total of 9 dogs underwent creation of MR. All animals survived the procedure. One animal was euthanized the first postoperative night after developing medically refractory sustained ventricular tachycardia and therefore was not included in the following analysis. Two additional animals that survived into the interval monitoring period were excluded from analysis. One animal was euthanized in the setting of acute fulminant heart failure, 4.2 months post survival surgery. The other animal was found to have near-total resolution of MR at the time of terminal surgery with only a

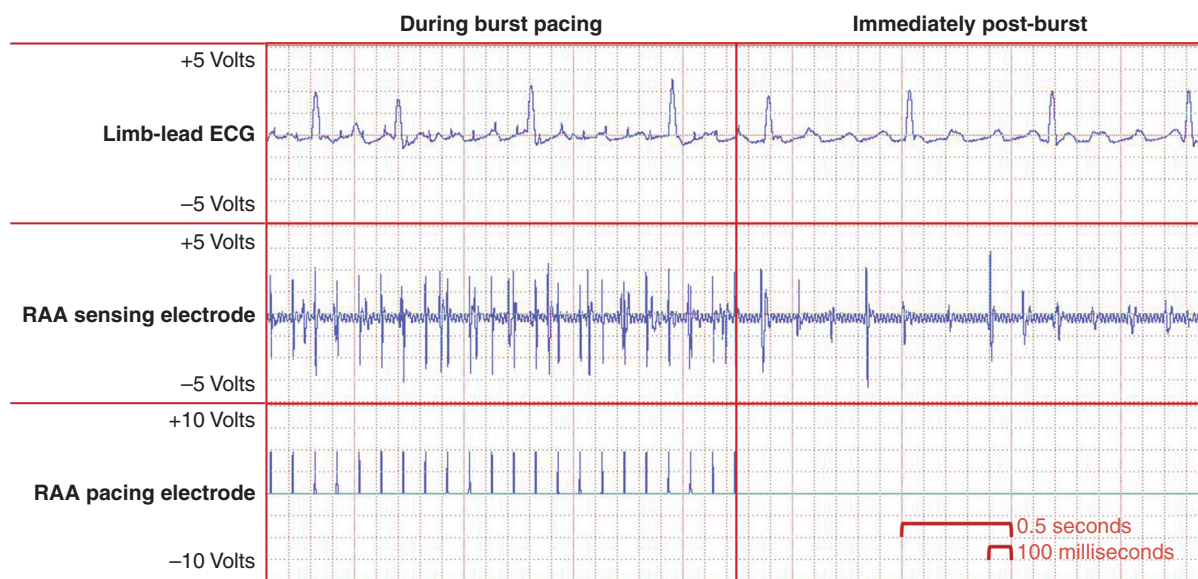


**FIGURE 3.** Assessment of atrial arrhythmogenic substrate via transvenous pacing of the right atrial appendage (RAA). Shown are representative electro-physiologic recordings made during a burst pacing attempt that successfully induced an atrial tachyarrhythmia, shown on the electrocardiogram (ECG) and the RAA-sensing electrode.

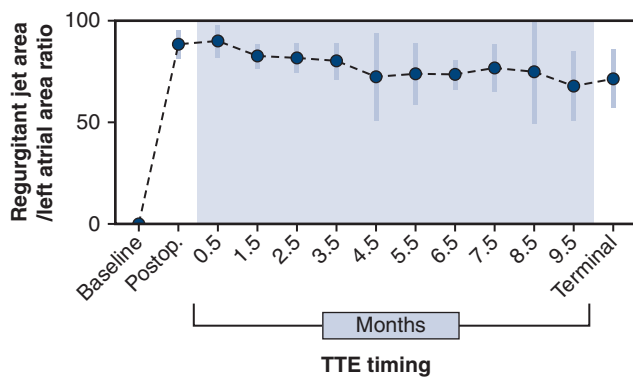


**FIGURE 4.** Echocardiographic measurement of mitral regurgitation (MR): MR remained severe over time. Regurgitant jet area-to-left atrial area (RJA/LAA) ratio (measured via transthoracic echocardiography [TTE]) plotted over the entire time course of the experimental protocol. Mean RJA/LAA values are shown with standard deviation bars. Blue shading indicates TTEs performed during the interval monitoring period, which was of a variable length for each dog. Severe MR was induced and maintained over an average period of 9 months.

trace, nonquantifiable MR jet. This animal had a 65% RJA/LAA immediately after MR creation.

The 6 dogs included in the following analysis maintained severe MR throughout the period of interval monitoring. Only 1 animal developed clinical signs of HF, with increased work of breathing with both exertion and lying in the lateral decubitus position. This animal was therefore treated with oral furosemide as described previously. Four dogs were female, 2 were male, and the mean duration with severe MR was  $8.6 \pm 1.6$  months. Mean age at terminal surgery was  $17.4 \pm 2.4$  months. Between the survival and terminal surgeries, dogs' weight and length increased, with mean increases of  $4.8 \pm 2.0$  kg ( $P = .002$ ) and  $12 \pm 8$  cm ( $P = .017$ ). Baseline MRI examinations were performed on average  $2.3 \pm 0.7$  weeks before survival surgery; preterminal MRI examinations were performed a mean of  $3.6 \pm 1.5$  weeks before terminal surgery.

**Quantification of MR.** No animal had MR on baseline TTE (Figure 4). Immediate postoperative TTE showed severe MR in all 6 dogs, with a mean RJA/LAA of  $88 \pm 7\%$ . Although the mean RJA/LAA at the time of terminal surgery was lower than immediately postoperatively ( $P = .044$ ), at  $71 \pm 14\%$  it remained severe, well surpassing the 50% threshold. Moreover, at the time of terminal surgery, all animals had either a flail leaflet and/or an eccentric wall-impinging jet (Table 1). Mean RF on terminal TEE was  $52 \pm 11\%$ .

**Volumetric changes to the left atrium.** There were marked structural changes to the LA over time. LA volume increased continuously over the interval monitoring period (Figures 5, and E1). As measured via TTE, mean baseline indexed LAV was  $21.6 \pm 6.7$  mL, and mean terminal indexed LAV more than doubled at  $56.0 \pm 27.8$  mL ( $P = .039$ ). The mean percentage increase in echo-derived LAV was  $163 \pm 147\%$ , with a range from 46% to 456%. As measured via MRI, mean baseline indexed LAV was  $37.7 \pm 10.5$  mL, and mean terminal indexed LAV was  $89.3 \pm 40.7$  mL ( $P = .011$ ). The mean percentage increase in MRI-derived LAV was  $132 \pm 54\%$  with a range from 58% to 220%.

**Volumetric changes to the LV.** The LV also underwent structural changes (Figures 5, and E1). Mean baseline indexed LVID was  $4.1 \pm 0.3$  cm, and mean terminal indexed LVID was  $4.8 \pm 0.9$  cm ( $P = .113$ ), with a mean percentage increase of  $15 \pm 19\%$ . The increase in LV end-diastolic volume (measured via MRI) was more marked, with a mean baseline indexed LV EDV of  $86.9 \pm 6.4$  mL and a mean terminal indexed LV EDV of  $119.5 \pm 19.2$  mL ( $P = .008$ ). The mean percentage increase in LV EDV was  $38 \pm 21\%$ .

When measured via TEE, LVEF decreased from a mean baseline EF of  $64 \pm 4\%$  to a mean terminal EF of  $57 \pm 6\%$  ( $P = .028$ ). Via MRI, mean baseline EF was  $53 \pm 7\%$ , and mean terminal EF was  $44 \pm 7\%$  ( $P = .082$ ). Via TEE, mean baseline indexed SV was  $32.2 \pm 2.4$  mL and mean terminal indexed SV was  $42.2 \pm 14.6$  mL ( $P = .137$ ). Via MRI, mean

**TABLE 1. Characterization of MR at time of terminal surgery**

Chronic study (n = 6)		
Animal	RJA/LAA via TTE	MR characteristics via TEE
1	60.3%	Two eccentric wall-impinging jets, A2 flail leaflet
2	71.7%	Central jet, ruptured chorda, major coaptation defect at A2/P2, A2/A3 flail leaflets
3	84.3%	Posteriorly directed eccentric wall-impinging jet, A2/A3 flail leaflets
4	51.3%	Posteriorly directed eccentric wall-impinging jet, A1 flail leaflet
5	89.6%	Eccentric wall-impinging jet, A2 flail leaflet
6	70.6%	Anteriorly directed eccentric wall-impinging jet, P2 flail leaflet
Mean (SD)	71.3% (14.3%)	

RJA/LAA, Regurgitant jet area to left atrial area ratio; MR, mitral regurgitation; TTE, transthoracic echocardiography; TEE, transesophageal echocardiography; SD, standard deviation.

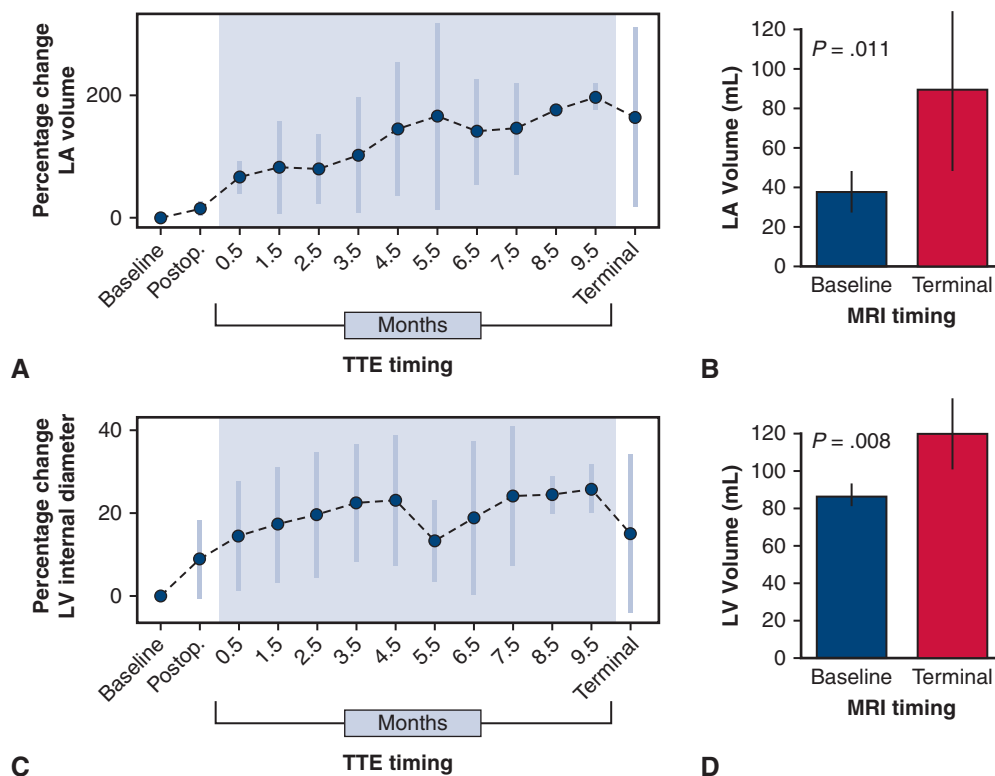


**FIGURE 5.** Echocardiographic and magnetic resonance imaging (MRI) measurements of volumetric changes to the left atrium (LA) and left ventricle (LV) that occurred over a mean duration of 9 months with severe mitral regurgitation (MR). All values shown were indexed to body surface area as measured at the time of exam, and are shown with standard deviation bars. A, LA volume as measured via transthoracic echocardiography (TTE). Blue shading indicates TTEs performed during the interval monitoring period, which was of a variable length for each dog. B, LA volume as measured via cardiac MRI. C, LV internal diameter as measured via TTE. Blue shading indicates TTEs performed during the interval monitoring period. D, LV end-diastolic volume, as measured via MRI.

baseline indexed SV was  $46.1 \pm 6.2$  mL, and mean terminal indexed SV was  $52.2 \pm 11.0$  mL ( $P = .337$ ).

**Assessment of atrial arrhythmogenic substrate.** An arrhythmogenic substrate developed in the majority of animals. None of the animals had an inducible ATA at baseline, immediately before the creation of MR. Four of 6 animals (67%) had an inducible ATA lasting >30 seconds at the time of terminal surgery, with a range of inducible ATAs lasting from 2.2 to 105 minutes (Table 2). Specific burst pacing settings for animals with and without inducible ATAs can be seen in Table 2. There were no significant hemodynamic changes/sustained hypotension during the induced ATAs.

**DISCUSSION**

A pilot study consisting of 4 dogs was used to develop a reproducible minimally invasive technique for the creation of severe MR via endovascular chordae avulsion. This technique was subsequently employed in a chronic survival study involving 9 study subjects. We had 2 mortalities, one from early ventricular arrhythmias and one from HF. Six dogs with severe MR completed the chronic study, with a mean duration of regurgitation of  $8.6 \pm 1.6$  months. The mean RJA/LAA at the time of terminal surgery was  $71 \pm 14\%$ , corresponding to a mean RF of  $52 \pm 11\%$ . Marked LAV increase was observed, with a mean echocardiographically measured LAV increase from

**TABLE 2.** Summary of transvenous burst pacing settings during terminal surgeries

Group	No. animals	Amplitude, mAmp	Period, milliseconds	No. bursts	ATA duration
All animals	6	0.6-3.0	80-135	1-6	6 s to 105 min
ATA inducible*	4	0.6-2.4	100-120	1-3	2.2-105 min
ATA not inducible	2	1.5-3.0	80-135	6	6-9 s

ATA, Atrial tachyarrhythmia. \*An ATA was considered inducible if it lasted for 30 s or longer.

baseline of  $163 \pm 147\%$  ( $P = .039$ ). LV EDV also increased, with a mean MRI-measured LV EDV increase from baseline of  $38 \pm 21\%$  ( $P = .008$ ). While LV function overall remained within or close-to normal limits, echocardiographically derived EF did decrease with a mean baseline EF of  $64 \pm 4\%$  and mean terminal EF of  $57 \pm 6\%$  ( $P = .028$ ). Four of 6 animals had inducible ATAs lasting >30 seconds at the time of terminal surgery. Overall, severe MR induced during survival surgery remained severe over the interval monitoring period, and led to LA and LV structural changes and increased electrical irritability of the atria.

### Similarities to the Human Phenotype of Severe MR

Increase in LAV, LVID, and LV EDV are all seen in patients with MR. The 2020 American Heart Association guidelines for valvular disease list LV dilation as evidence of severe MR.<sup>22,23</sup> In an echocardiographic study performed in 116 patients with MR and 52 controls, Cameli and colleagues<sup>24</sup> found that patients with severe MR (defined as RF greater or equal to 50%) had significantly greater mean indexed LAV than control patients and patients with mild and moderate MR. The mean percentage difference in indexed LAV in patients with severe MR compared with controls in their study was 48%. LA dilation was also seen in our canine study, but was more marked with increases in LAV between 132% and 163% depending on imaging modality. Cameli and colleagues<sup>24</sup> found a nonsignificant trend of larger LVID in patients with severe MR compared with controls, with a mean percent difference of 7%. LVID increase over time in our study was 15%. Denney and colleagues<sup>25</sup> found that patients with moderate-to-severe chronic primary MR had an average of 59% greater MRI-derived LV EDV than control patients. In our study, the mean increase in LV EDV was 38%.

Our canine model reproduced human pathophysiologic findings of LA and LV remodeling, and accomplished this within an abbreviated timeframe in comparison with the typical clinical scenario.<sup>26</sup> This extensive remodeling was seen with few appreciable clinical signs of HF. Of the 8 dogs that survived the immediate period after MR creation, only one dog died of acute HF before completing all study protocols. Of the 6 animals that underwent the full study with sustained severe MR, just one showed clinical signs of HF, which resolved with oral furosemide. This particular animal had a 456% increase in indexed LAV, a 42% increase in indexed LVID, and a 69% increase in indexed LV EDV. This model represents an opportunity to study physiology that is commensurate with human disease, in which the majority of animals are either asymptomatic, or minimally symptomatic and easily managed with oral medication.

This study also reproduced human pathophysiologic findings of ATA-inducibility in patients with severe MR.

While observational studies in humans have shown up to 48% of patients with MR developing AF by 10 years from diagnosis,<sup>6</sup> in our study 67% of dogs had inducible ATAs at time of terminal surgery after just 9 months. This replicates the variability seen in human practice, in which not all patients with severe MR go on to develop ATAs.<sup>22</sup> It is our hope that this model will provide a window into understanding this phenomenon, and help define the specific anatomic and electrophysiological substrates that are needed to develop sustained AF.

### Choice of Echocardiographic Parameters for Severe MR

While RF, regurgitant volume, and effective regurgitant orifice area are commonly used in the clinical setting, RJA/LAA has been proposed as the best and most reproducible quantitative measurement of MR in canines.<sup>19</sup> RJA/LAA additionally has advantages over traditional clinical measurements. Most importantly, it avoids the geometrical assumption fundamental to the proximal isovelocity surface area method, ie, that the regurgitant orifice is circular and therefore the most proximal area of the jet has a hemispherical distribution of velocity factors.<sup>27</sup> This geometric assumption is often not met in the case of a flail or torn leaflet, with resultant eccentric wall-impinging MR jet and noncircular regurgitant orifice, as was often the case in our model.

RJA/LAA is used clinically, although less often than in veterinary medicine. The 2017 American Society of Echocardiography guideline on noninvasive evaluation of native valvular regurgitation lists a RJA/LAA of >50% or a wall-impinging eccentric MR jet (of variable size) to be consistent with severe MR.<sup>20</sup> It is also important to note that these guidelines list flail leaflet as specific for severe MR.

Generally, canine echocardiographic parameters for grading of structural and functional disease cannot be as precise as those used in humans given the extreme differences in size and shape of dogs of various breeds.<sup>28,29</sup> One observational study performed in a variety of small dog breeds in which MR natively developed showed that dogs with asymptomatic MR had a mean RJA/LAA of  $41 \pm 10\%$  (SD) and dogs with clinical signs of HF had a mean RJA/LAA of  $58 \pm 13\%$ .<sup>19</sup> In our study, a mean RJA/LAA of 71% was generally associated with severe asymptomatic MR.

Due to the geometric differences of human versus canine thoracic anatomy, not all views used in standard human echocardiography are possible in dogs, particularly via TTE. It was only technically feasible to achieve adequate-quality imaging necessary for calculation of RF and LVEF via TEE. TTE was chosen over TEE for interval monitoring to minimize invasiveness and allow for evaluations without anesthesia.

### Comparison With Other Large Animal Models of MR—Echocardiography and MRI

Although other large animal models of MR have been described, most were more invasive, and few rigorously applied echocardiographic or MRI analysis. Among published studies that used similar canine models of endovascularly created MR, we have only found 2 that used echocardiography to determine adequate severity of MR, with neither listing specific quantifiable criteria.<sup>14,15</sup> One of these groups reported changes in LAV over time, with a mean increase of 105% at 1 month after MR creation.<sup>14</sup> This is in comparison with a mean LAV increase of 163% in our study. This group also measured LV remodeling via TTE-derived LV fractional shortening and found no significant change in this measure, and, indeed, a return to baseline by the termination of the study. Comparatively, we used TEE-derived LVEF, which is considered a more robust measure of LV function,<sup>30</sup> and found that LVEF decreased from  $64 \pm 4\%$  (standard deviation) to  $57 \pm 6\%$  ( $P = .028$ ). Neither of the earlier studies quantitatively reported the severity of MR at time of terminal surgery.

Among published studies that used similar canine models of endovascularly created MR, we have found only one group that used MRI volumetric assessment, focusing on assessment of the LV and not the LA.<sup>31</sup> This group did not quantitate the severity of induced MR.

Li and colleagues<sup>32</sup> more recently reported a porcine model of MR created via open-chest mitral chordae avulsion (through a purse-string in the LA appendage) in which echocardiography was used in a rigorous fashion. This group used a RJA/LAA  $>40\%$  as the threshold for severe MR. Of the 8 pigs that met these criteria at the time of terminal surgery (30 months after MR creation), mean RJA/LAA was  $47 \pm 2\%$  (mean  $\pm$  standard error of the mean), and end-systolic LAV increased from a mean of  $12.1 \pm 1.5$  mL at baseline to  $33.1 \pm 2.3$  mL at time of terminal surgery, corresponding to a 174% increase in LAV. Most of this increase was seen in the first 6 months after MR creation. This group also examined LV remodeling, via TTE-derived LV EDV and LVEF. They found a significant increase of 40% in LV EDV but no change in LVEF, with mean baseline and mean terminal LVEF both 69%. Measurement of LV EDV and LVEF were not reliable via TTE in our dogs; we observed an increase in MRI-derived LV EDV and TEE-derived LVEF, but little change in MRI-derived LVEF.

The results of Li and colleagues<sup>32</sup> overall agree with ours, although their methodology had the notable difference of the prophylactic administration of a daily regimen of digoxin, furosemide, spironolactone, and potassium citrate to all pigs for 1 month after MR creation. Moreover, opening the chest and pericardium greatly complicates not only the procedure and recovery but also confounds assessment

of LA function. Our group has previously shown in a porcine model that performing a sternotomy and pericardiotomy alone is associated with a significant increase in LAV and decrease in LA booster pump function at 30 days postoperatively.<sup>33</sup> It is therefore crucial to avoid pericardial disruption when assessing the effect of an intervention on atrial function.

### Comparison With Other Large Animal Models of MR—Assessment of Atrial Arrhythmogenic Substrate

Inducibility of ATAs was assessed in the 3 large animal MR models listed previously (2 canine and 1 porcine). Verheule and colleagues<sup>14</sup> reported inducibility of AF lasting longer than 60 minutes in 10 of 19 dogs (53%) at 1 month post-MR creation; Sun and colleagues<sup>15</sup> reported induced ATAs lasting longer than 5 minutes in 4 of 5 dogs (80%) at 3 months. Neither group quantified the degree of MR at the time of terminal surgery. Li and colleagues<sup>32</sup> found that among pigs with severe MR (defined as RJA/LAA  $>40\%$ ) at the time of terminal surgery, 4 of 8 (50%) had an inducible ATA lasting longer than 3 minutes. In our study, 4 of 6 dogs (67%) had inducible ATAs lasting longer than 30 seconds at a mean of 9 months post-MR creation, with severe MR defined as RJA/LAA  $>50\%$ , and with a range of inducible ATAs lasting from 2.2 to 105 minutes. Our canine model of MR combined robust imaging surveillance and quantification (via TTE, TEE, and MRI) with a rate of acquired inducibility of ATAs that is similar to previous animal models that lacked this robust quantification.

### Comparison of Echocardiographic and MRI Results

Multiple variables, including volume status and preload, can significantly affect the measurement of cardiac function and specifically MR.<sup>20</sup> This is more likely to be an issue when comparing results of images taken at different times and under different conditions (eg, awake vs sedated). In this study, terminal MRI examinations were performed on average 3.6 weeks before terminal TTE and TEE. Therefore, it is not surprising that our echocardiographic and MRI measurements were not identical. They did, however, generally agree in terms of trends over time. LAV showed the most marked change, increasing from baseline to terminal surgery by both TTE and MRI measurements ( $P = .039$  and  $.011$ , respectively). LV chamber size increased more notably as measured by MRI (LV EDV,  $P = .008$ ) than by TTE (LVID,  $P = .113$ ), whereas LVEF decreased more notably by TEE than MRI ( $P = .028$  and  $.082$ , respectively). Together, the 3 imaging modalities of TTE, TEE, and MRI supported that severe MR led to remodeling of both the LA and LV, with the most substantial changes seen in the left atrium.



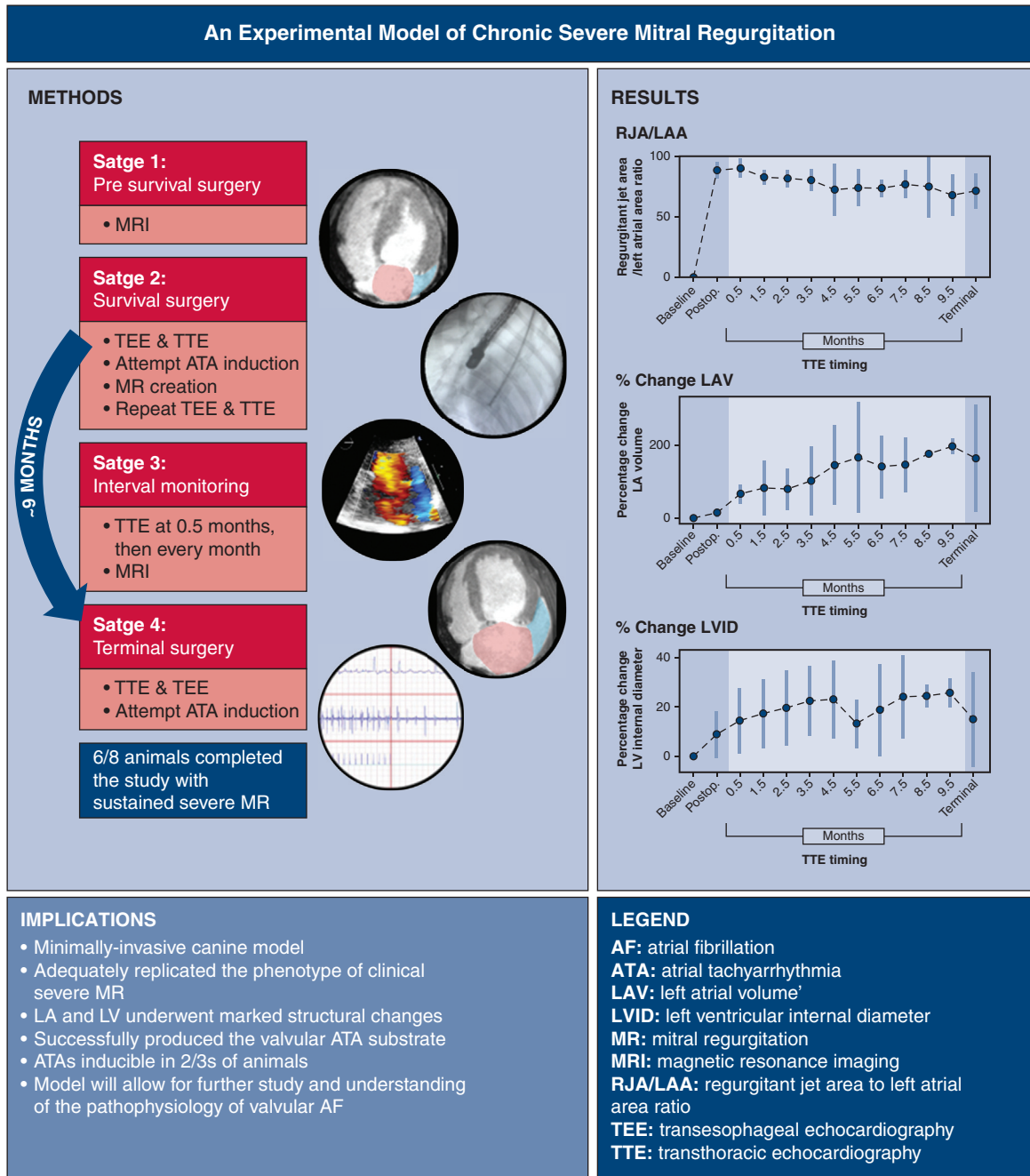


**FIGURE 6.** Graphical abstract: an experimental model of chronic severe mitral regurgitation. *RJA*, Regurgitant jet area; *LAA*, left atrial area; *MRI*, magnetic resonance imaging; *TEE*, transesophageal echocardiography; *TTE*, transthoracic echocardiography; *MR*, mitral regurgitation; *LAV*, left atrial volume; *LVID*, left ventricular end-diastolic internal diameter ; *ATA*, atrial tachyarrhythmia; *LV*, left ventricle; *LA*, left atrium; *AF*, atrial fibrillation.

**Limitations**

Although this model represents a significant improvement when compared with previous large animal models

of MR, it also has limitations. Mechanical creation of MR is necessarily artificial and cannot replicate whatever factors lead to native development of clinical primary MR.

In addition, we cannot provide a sense of the incidence or potential burden of spontaneously arising ATAs in these animals, as they did not tolerate continuous Holter-monitoring without sedation.

Finally, severe sustained MR was not achieved in all animals—1 of 7 dogs that survived until terminal surgery had resolution of MR. However, this was early in our experience (the second consecutive animal in the chronic study), and an 86% success rate is still excellent. Most published canine models of MR have not reported the percentage of dogs that failed to sustain MR, so we cannot compare the relative success of our models. Two canine studies did report this metric (both from the same group): they defined chronic severe MR as RF >50% for greater than 3 months as measured via a combination of thermodilution and angiography, and reported a 69% to 90% success rate.<sup>9,10</sup> Although catheter-based measurements of MR were acceptable at the time (the late 1980s), they would not be adequate today. In a more recent porcine model, Li and colleagues<sup>32</sup> reported an 89% success rate of sustaining MR. However, their mean terminal RJA/LAA was 47%, which would fail to pass the threshold for severe MR of >50% in our study. Although there was a single surgeon who created MR in our study, and therefore we cannot characterize the learning curve for other operators, it is notable that we were able to operatively achieve the 50% RJA/LAA threshold for severe MR in all animals (both in the pilot and chronic studies) without issue.

A further limitation of this study is the small sample size of 6 animals that completed the entire study protocol. However, the goal of this study was to create a robust model that could be used for further study, and accordingly we are actively using this model in ongoing experimental studies.

## CONCLUSIONS

This minimally invasive canine model successfully reproduced the clinical phenotype of severe MR. This phenotype was rigorously defined and was both reproducible and well-tolerated by most animals. Therefore, further use of this model may offer opportunities to better understand the effects of severe MR and the resultant atrial and ventricular remodeling. Our results suggest that this model will enable a precise definition of the substrate for MR-induced ATAs (Figure 6).

## Conflict of Interest Statement

R.J.D. reported AtriCure, Inc: speaker and receives research funding; Medtronic: consultant and receives research funding; and Edwards Lifesciences: consultant and receives research funding. All other authors reported no conflicts of interest.

The *Journal* policy requires editors and reviewers to disclose conflicts of interest and to decline handling or reviewing manuscripts for which they may have a conflict

of interest. The editors and reviewers of this article have no conflicts of interest.

## References

- Coffey S, Roberts-Thomson R, Brown A, Carapetis J, Chen M, Enriquez-Sarano M, et al. Global epidemiology of valvular heart disease. *Nat Rev Cardiol*. 2021;18:853-64.
- Tsao CW, Aday AW, Almarzooq ZI, Alonso A, Beaton AZ, Bittencourt MS, et al. American Heart Association Council on Epidemiology and Prevention Statistics Committee and Stroke Statistics Subcommittee. Heart disease and stroke statistics—2022 update: a report from the American Heart Association. *Circulation*. 2022;145:e153-639.
- GBD 2019 Diseases and Injuries Collaborators. Global burden of 369 diseases and injuries in 204 countries and territories, 1990-2019: a systematic analysis for the Global Burden of Disease Study 2019. *Lancet*. 2020;396:1204-22.
- de Marchena E, Badiye A, Robalino G, Junttila J, Atapattu S, Nakamura M, et al. Respective prevalence of the different Carpentier classes of mitral regurgitation: a stepping stone for future therapeutic research and development. *J Card Surg*. 2011;26:385-92.
- Badhwar V, Rankin JS, Damiano RJ Jr, Gillinov AM, Bakaeen FG, Edgerton JR, et al. The Society of Thoracic Surgeons 2017 clinical practice guidelines for the surgical treatment of atrial fibrillation. *Ann Thorac Surg*. 2017;103:329-41.
- Grigioni F, Avierinos JF, Ling LH, Scott CG, Bailey KR, Tajik AJ, et al. Atrial fibrillation complicating the course of degenerative mitral regurgitation: determinants and long-term outcome. *J Am Coll Cardiol*. 2002;40:84-92.
- Dell'Italia LJ, Meng QC, Balcells E, Straeter-Knowlen IM, Hanks GH, Dillon R, et al. Increased ACE and chymase-like activity in cardiac tissue of dogs with chronic mitral regurgitation. *Am J Physiol*. 1995;269:H2065-73.
- Dell'Italia LJ, Balcells E, Meng QC, Su X, Schultz D, Bishop SP, et al. Volume-overload cardiac hypertrophy is unaffected by ACE inhibitor treatment in dogs. *Am J Physiol*. 1997;273:H961-70.
- Kleaveland JP, Kussmaul WG, Vinciguerra T, Deters R, Carabello BA. Volume overload hypertrophy in a closed-chest model of mitral regurgitation. *Am J Physiol*. 1988;254:H1034-41.
- Carabello BA, Nakano K, Corin W, Biederman R, Spann JF Jr. Left ventricular function in experimental volume overload hypertrophy. *Am J Physiol Heart Circ Physiol*. 1989;256:H974-81.
- Choi H, Lee K, Lee H, Lee Y, Chang D, Eom K, et al. Quantification of mitral regurgitation using proximal isovelocity surface area method in dogs. *J Vet Sci*. 2004;5:163-71.
- Oyama MA, Sisson DD, Bulmer BJ, Constable PD. Echocardiographic estimation of mean left atrial pressure in a canine model of acute mitral valve insufficiency. *J Vet Intern Med*. 2004;18:667-72.
- Cox JL, Canavan TE, Schuessler RB, Cain ME, Lindsay BD, Stone C, et al. The surgical treatment of atrial fibrillation: II. Intraoperative electrophysiologic mapping and description of the electrophysiologic basis of atrial flutter and atrial fibrillation. *J Thorac Cardiovasc Surg*. 1991;101:406-26.
- Verheule S, Wilson E, Everett T IV, Shanbhag S, Golden C, Olgin J. Alterations in atrial electrophysiology and tissue structure in a canine model of chronic atrial dilatation due to mitral regurgitation. *Circulation*. 2003;107:2615-22.
- Sun Q, Tang M, Pu J, Zhang S. Pulmonary venous structural remodeling in a canine model of chronic atrial dilatation due to mitral regurgitation. *Can J Cardiol*. 2008;24:305-8.
- Guichard JB, Naud P, Xiong F, Qi X, L'Heureux N, Hiram R, et al. Comparison of atrial remodeling caused by sustained atrial flutter versus atrial fibrillation. *J Am Coll Cardiol*. 2020;76:374-88.
- Goldstein RN, Ryu K, Khrestian C, van Wagoner DR, Waldo AL. Prednisone prevents inducible atrial flutter in the canine sterile pericarditis model. *J Cardiovasc Electrophysiol*. 2008;19:74-81.
- Clauss S, Bleyer C, Schüttler D, Tomsits P, Renner S, Klymiuk N, et al. Animal models of arrhythmia: classic electrophysiology to genetically modified large animals. *Nat Rev Cardiol*. 2019;16:457-75.
- Muzzi RA, de Araújo RB, Muzzi LA, Pena JL, Silva EF. Regurgitant jet area by Doppler color flow mapping: quantitative assessment of mitral regurgitation severity in dogs. *J Vet Cardiol*. 2003;5:33-8.
- Zoghbi WA, Adams D, Bonow RO, Enriquez-Sarano M, Foster E, Grayburn PA, et al. Recommendations for noninvasive evaluation of native valvular regurgitation: a report from the American Society of Echocardiography developed in Collaboration with the Society for Cardiovascular Magnetic Resonance. *J Am Soc Echocardiogr*. 2017;30:303-71.

21. Cowgill GR, Drabkin DL. Determination of a formula for the surface area of the dog together with a consideration of formulae available for other species. *Am J Physiol.* 1927;81:36-61.
22. Goldstone Woo. Surgical treatment of the mitral valve. *Sabiston and Spencer Surgery of the Chest.* 9th ed St. 2016.
23. Otto CM, Nishimura RA, Bonow RO, Carabello BA, Erwin JP 3rd, Gentile F, et al. 2020 ACC/AHA guideline for the management of patients with valvular heart disease: a report of the American College of Cardiology/American Heart Association Joint Committee on clinical practice guidelines. *Circulation.* 2021; 143:e72-227.
24. Cameli M, Lisi M, Giacomini E, Caputo M, Navarri R, Malandrino A, et al. Chronic mitral regurgitation: left atrial deformation analysis by two-dimensional speckle tracking echocardiography. *Echocardiography.* 2011;28:327-34.
25. Denney TS Jr, Nagaraj HM, Lloyd SG, Aban I, Corros C, Seghatol-Eslami F, et al. Effect of primary mitral regurgitation on left ventricular synchrony. *Am J Cardiol.* 2007;100:707-11.
26. Zilberszac R, Heinze G, Binder T, Laufer G, Gabriel H, Rosenhek R. Long-Term outcome of active surveillance in severe but asymptomatic primary mitral regurgitation. *JACC Cardiovasc Imaging.* 2018;11:1213-21.
27. Ziani AB, Latcu DG, Abadir S, Paranon S, Dulac Y, Guerrero F, et al. Assessment of proximal isovelocity surface area (PISA) shape using three-dimensional echocardiography in a paediatric population with mitral regurgitation or ventricular shunt. *Arch Cardiovasc Dis.* 2009;102:185-91.
28. della Torre PK, Kirby AC, Church DB, Malik R. Echocardiographic measurements in greyhounds, whippets and Italian greyhounds—dogs with a similar conformation but different size. *Aust Vet J.* 2000;78:49-55.
29. Vörös K, Hetey C, Reiczigel J, Czirik GN. M-mode and two-dimensional echocardiographic reference values for three Hungarian dog breeds: Hungarian Vizsla, Mudi and Hungarian greyhound. *Acta Vet Hung.* 2009;57:217-27.
30. Lang RM, Badano LP, Mor-Avi V, Afilalo J, Armstrong A, Ernande L, et al. Recommendations for cardiac chamber quantification by echocardiography in adults: an update from the American Society of Echocardiography and the European Association of Cardiovascular Imaging. *Eur Heart J Cardiovasc Imaging.* 2015;16:233-71.
31. Pat B, Killingsworth C, Denney T, Zheng J, Powell P, Tillson M, et al. Dissociation between cardiomyocyte function and remodeling with  $\beta$ -adrenergic receptor blockade in isolated canine mitral regurgitation. *Am J Physiol Heart Circ Physiol.* 2008;295:H2321-7.
32. Li B, Cui Y, Zhang D, Luo X, Luo F, Li B, et al. The characteristics of a porcine mitral regurgitation model. *Exp Anim.* 2018;67:463-77.
33. Voeller RK, Zierer A, Lall SC, Sakamoto SI, Chang NL, Schuessler RB, et al. The effects of the Cox maze procedure on atrial function. *J Thorac Cardiovasc Surg.* 2008;136:1257-64. 1264.e1-3.

**Key Words:** translational research, mitral regurgitation, atrial fibrillation, arrhythmias, echocardiography, cardiac magnetic resonance imaging, large animal model

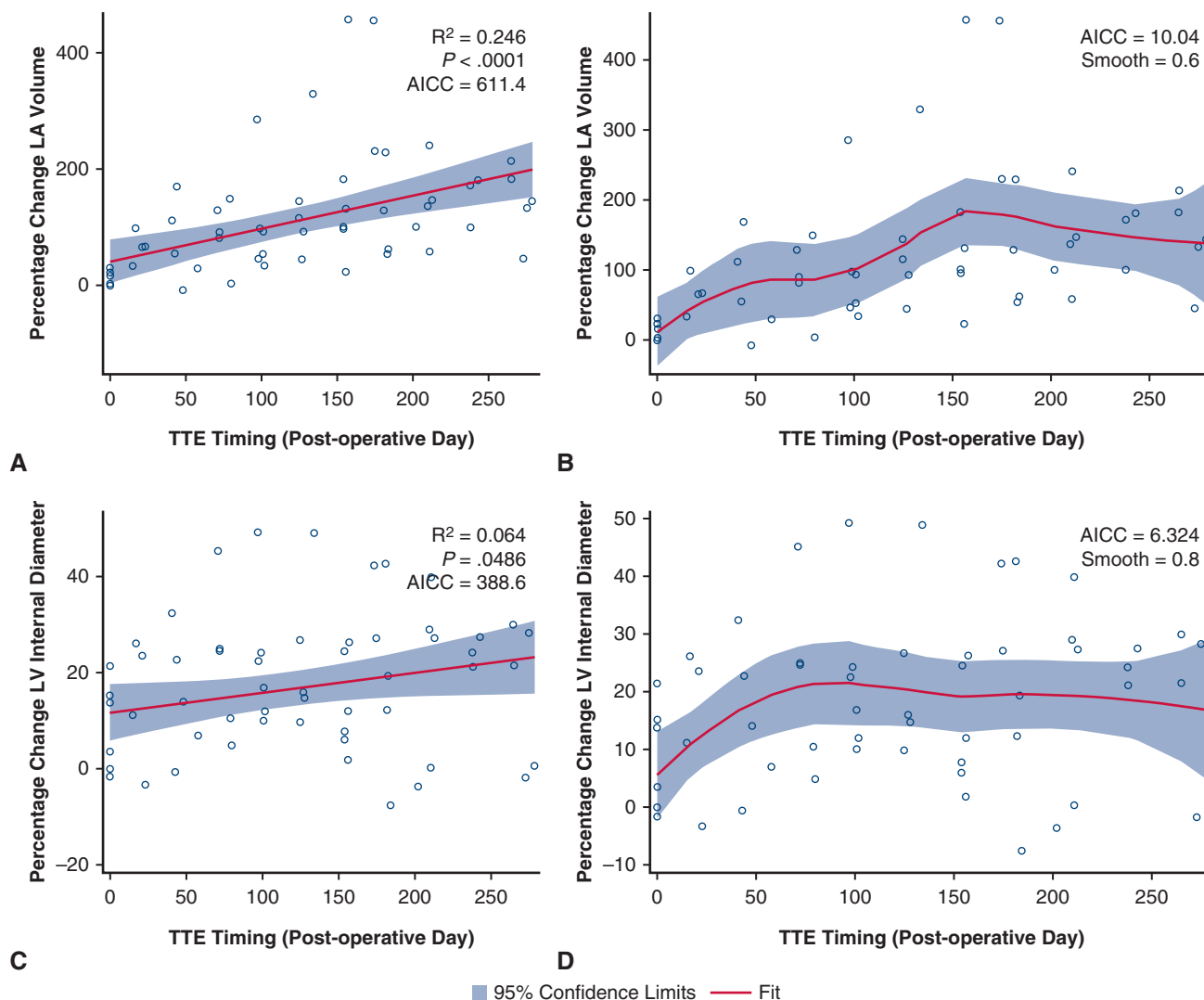


**FIGURE E1.** Models of left atrial and left ventricular remodeling over time. A and B model percentage change in indexed left atrial (LA) end-systolic volume as measured via transthoracic echocardiography (TTE) versus time since creation of mitral regurgitation (MR); C and D model percentage change in left ventricular end-diastolic internal diameter (LVID) as measured via TTE versus time since MR creation. A and C show simple linear regression models, with the following parameters reported: coefficient of determination ( $R^2$ ),  $P$  value as compared with no correlation between percentage change and time since mitral regurgitation (MR) creation, and Akaike information criterion corrected for small sample size (AICC). B and D show locally estimated scatterplot smoothing (LOESS) models, with the following parameters reported: AICC and the smoothing parameter used (smooth). It is possible to perform a simple linear regression to compare time since MR-creation with either left atrial volume (LAV) or LVID. However, in this sample, LAV and LVID are not normally distributed (and therefore should not be modeled using a parametric test). We can use a nonparametric method such as LOESS, which does not make any assumptions about the underlying structure of the data, and uses local regression to fit a smooth curve through a scatterplot of data. It is possible to calculate the coefficient of determination ( $R^2$ ) for simple linear regression lines for both LAV and LVID, and although both show positive correlation between the outcome variables and time since MR creation (ie,  $P < .05$ ), said correlation is weak, with  $R^2$ s of just 0.2416 and 0.0643, respectively. We have also shown LOESS models for both variables, which relative to the linear regression models are better representations of the data. This can be seen in the relative AICC of the linear regression versus LOESS models—AICC is a relative measure of goodness of fit, with a lower AICC for a specific outcome variable and its predictor variables indicating better fit (LAV and LVID AICC by definition cannot be compared). For both outcome variables LAV and LVID, AICC of the LOESS model is at least an order of magnitude smaller than for the simple linear regression model (LAV linear AICC 611.4, LOESS AICC 10.04; LVID linear AICC 388.6, LOESS AICC 6.324). Also of note, because LOESS is a nonparametric model and because there is no comparator group in this model-development study, there is no associated  $P$  value. There are multiple other complex statistical methods that could be used to model this data, including those that would take into account the nonindependence of repeated measures data, but we are limited in use of these tests by the small overall sample size and the potential for overfitting. *LV*, Left ventricular.

**TABLE E1. Animal characteristics in the acute pilot study (n = 4)**

% Female	100%
Age, mo, mean $\pm$ SD	14.4 $\pm$ 4.0
Weight, kg, mean $\pm$ SD	26.7 $\pm$ 1.7

*SD*, Standard deviation.

**TABLE E2. Characterization of MR in the acute pilot study**

Acute pilot study (n = 4)			
Animal	RJA/LAA via TTE	MR characteristics via TEE	Gross valve pathology
P1	57.6%	One eccentric wall-impinging jet, one central jet	Anterior leaflet trauma
P2	83.0%	Posterior flail leaflet	Ruptured chorda and posterior flail segment
P3	66.6%	Two eccentric wall-impinging jets	Ruptured chorda and posterior flail segment, torn anterior leaflet with flail of torn area
P4	89.0%	Two eccentric wall-impinging jets	Anterior and posterior leaflet trauma
Mean (SD)	74.1% (14.5%)		

*RJA/LAA*, Regurgitant jet area to left atrial area ratio; *TTE*, transthoracic echocardiography; *MR*, mitral regurgitation; *TEE*, transesophageal echocardiography; *SD*, standard deviation.